



PAPER

Potential of first row transition metal decorated graphtriene quantum dots as single atom catalysts towards hydrogen evolution reaction (HER)

RECEIVED
22 June 2023REVISED
27 September 2023ACCEPTED FOR PUBLICATION
10 October 2023PUBLISHED
19 October 2023Faizan Ullah¹ , Mazhar Amjad Gilani² , Muhammad Imran³, Khurshid Ayub¹ and Tariq Mahmood^{1,4} ¹ Department of Chemistry, COMSATS University Islamabad, Abbottabad Campus, Abbottabad-22060, Pakistan² Department of Chemistry, COMSATS University Islamabad, Lahore Campus, Lahore, Pakistan³ Department of Chemistry, Faculty of Science, King Khalid University, PO Box 9004, Abha 61413, Saudi Arabia⁴ Department of Chemistry, College of Science, University of Bahrain, Sakhir PO Box 32038, BahrainE-mail: mahmood@cuiatd.edu.pk and khurshid@cuiatd.edu.pk

Keywords: single atom catalyst, HER, graphtriene, DFT

Abstract

To advance the clean energy systems based on hydrogen, highly efficient and low-cost electrocatalysts for the hydrogen evolution reaction (HER) are of paramount importance. In recent years, single atoms embedded within 2-dimensional (2D) material substrates have emerged as exceptional catalysts for HER. Graphtriene, a 2D material due to its novel electronic properties is a promising substrate for development of single atom catalysts. In this study, we employed density functional theory (DFT) simulations to investigate the potential of transition metals (Fe, Co, Ni, Cu, and Zn) anchored on graphtriene quantum dot as single atom catalysts (SACs) for HER. Our results revealed that Zn and Ni SACs anchored on graphtriene quantum dot exhibit excellent HER performance. Additionally, we calculated total density of states (TDOS), partial density of states (PDOS), HOMO, LUMO energies and HOMO–LUMO energy gap for the proposed SACs. Our work presents a promising approach for the development of HER catalysts, utilizing graphtriene quantum dot as support material and transition metal atoms (Fe, Co, Ni, Cu, and Zn) as the single atom centers.

1. Introduction

To resolve environmental issues such as water contamination and air pollution, significant focus has been devoted to finding renewable energy sources to replace fossil fuels [1–4]. Hydrogen is considered an excellent replacement due to its environmental friendliness and high calorific value [5, 6]. For the purpose of efficient production of hydrogen, highly efficient hydrogen evolution reaction (HER) electrocatalysts, such as those with high activity and long-term stability are required [7–9]. Although platinum is considered as the most effective catalyst to facilitate HER, it is impractical for large-scale application. This is because of resource scarcity and high cost of platinum [10–12]. Therefore, cheaper high-performance HER catalysts devoid of noble metals are urgently required [13–15]. Transition metal-based catalysts, like transition metal phosphides [16, 17], transition metal chalcogenides [18–22], and transition metal nitrides [23–25], have been shown to be electrochemically active toward HER. However, their HER performance is currently inferior to that of Pt-based catalysts. Consequently, it is of the utmost importance to enhance the activity of noble metal free catalysts for HER.

Single-atom catalysts (SACs) have attracted considerable interest in recent years due to their increased activity and selectivity [26–29]. Two-dimensional nanosheets have unique structures and tunable electronic properties which make them promising substrates for SACs [30–33]. The hybridization between the d-orbitals of the embedded transition metals and the p-orbitals of the main group elements of the substrate has been proved to be a viable technique for increasing catalytic performance [34–37]. Recently, Single atoms, such as Co, Rh, and Ir, anchored on porphyrin-like graphene exhibited better CO₂ reduction catalytic activity [38].

Graphene-supported Cu nanoparticles have been reported to greatly enhance CO₂ conversion compared to the Cu(111) [39].

Graphtriyne (GTY) is a 2D carbon material in which each benzene ring is connected to each of six others through a chain formed of three acetylenic linkages [40]. With the correct pore size and acetylene bond, metal atoms may be stably incorporated in GTY.

In this study, we aim to investigate the electrocatalytic performance of transition metal atoms anchored on graphtriyne quantum dot support (TM@GTY) as single atom catalysts for the hydrogen evolution reaction (HER). Utilizing transition metal atoms (Fe, Co, Ni, Cu and Zn) embedded in the pores of graphtriyne quantum dot, we designed a series of single atom catalysts and examined their performance for HER using first principles density functional theory simulations. The outcomes of our work are anticipated to furnish a deeper understanding of the potential for developing highly efficient and cost-effective single atom catalysts for the hydrogen evolution reaction (HER). The results from this study will be valuable in guiding the exploration of new catalysts for hydrogen production and identifying the most promising candidates for further experimentation and development.

2. Computational methodology

All quantum chemical calculations were performed using density functional theory with ORCA 5.0 program package [41, 42]. The geometric relaxations and vibrational analysis of all structures were carried out at spin-polarized density functional theory using ω B97X-D3 hybrid functional [43] and triple- ζ basis set def2-TZVP, [44] together with the RIJCOSX approximation and the auxiliary basis set def2/J [45, 46]. The convergence tolerances for the geometry optimization were as follows: energy change = 5.0×10^{-6} Eh, maximal gradient = 3.0×10^{-4} Eh/Bohr, RMS gradient = 1.0×10^{-4} Eh/Bohr, maximal displacement = 4.0×10^{-3} Bohr, and RMS displacement = 2.0×10^{-4} Bohr. The ω B97X-D3 functional incorporates improved dispersion and long-range corrections and was selected to account for noncovalent interactions. From vibrational analysis it was ascertained that no imaginary frequencies in the optimized geometries. Then the optimized geometries were further subjected to single point energies calculations at PWPB95-D3/def2-TZVPP level of theory [47] utilizing the RIJCOSX approximation for Coulomb and Hartree–Fock exchange with the def2/J and def2-TZVPP/C auxiliary basis sets [48]. In order to achieve highly accurate energies, we employed the double hybrid meta-GGA density functional theory (DFT) functional PWPB95-D3 for single point energy simulations. This functional has been shown to provide exceptional accuracy in energy predictions, [49] making it an ideal choice for our calculations. The atom-pairwise dispersion correction was applied in all calculations using the Becke–Johnson damping scheme (D3BJ), as prescribed by Grimme *et al* [50, 51] This was implemented to enhance the reliability of our simulations, particularly in capturing van der Waals interactions. Multiwfn [52] was used to generate density of states (DOS) spectra and VMD [53] was employed for visualization of the molecular orbitals.

3. Results and discussion

As depicted in figure 1, the graphtriyne quantum dot, which consists of the formula C₅₄H₁₄, has been optimized by terminating its edges with hydrogen atoms to mitigate the impact of dangling bonds thereby significantly stabilizing the structure. It is worth noting that omitting this step of hydrogen termination would lead to the presence of highly reactive unpaired electrons associated with the carbon atoms at the edges [54]. These dangling bonds could introduce localized states within the energy gap, which would potentially disrupt the electronic properties and induce non-negligible deviations in the performance of the quantum dot. Such deviations could manifest as higher reactivity. Moreover, the absence of hydrogen termination could compromise thermodynamic stability. Therefore, hydrogen termination serves as a vital step in the design of a stable and functionally reliable graphtriyne quantum dot. [55] The initial geometry of graphtriyne quantum dot was designed in Avogadro software [56]. After geometry optimization, the structure of the graphtriyne quantum dot exhibits four distinct C–C bonds. These are the C(sp)–C(sp) bond (between two adjacent triple bonds), which has a computed bond length of 1.37 Å; aromatic C(sp²)–C(sp²) bond (1.40 Å); C(sp²)–C(sp) bond (1.42 Å); and the triple bonds with computed bond length of 1.20 Å. These calculated bond lengths of our designed graphtriyne quantum dot are in close agreement with graphtriyne unit cell derived from periodic DFT simulations reported in the existing literature [57, 58]. To design SACs, the metal atom (Fe, CO, Ni, Cu, and Zn) was embedded in the graphtriyne pore without disturbing the optimized structure of the pristine graphtriyne substrate. First, spin polarized DFT calculations were carried out in order to identify which spin state of the transition metal doped graphtriyne (TM@GTY) SACs is the most stable. Structures with the lowest energy, i.e., the most stable ones, were then subjected to further investigation in this work. The relative stabilities of the different spin states of Fe–Zn doped on graphtriyne quantum dot are shown in table 1. Fe@GTY prefers quintet spin state multiplicity

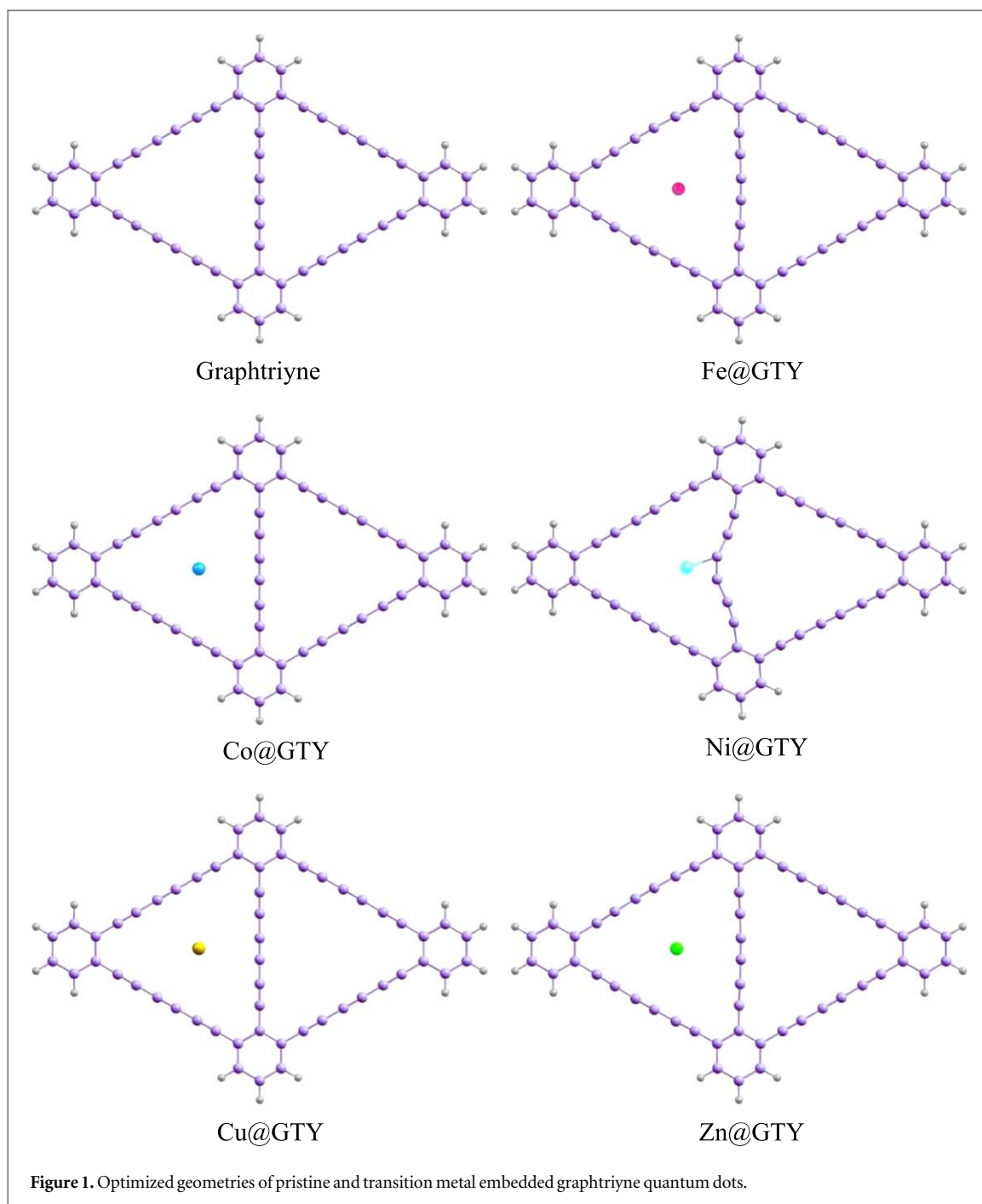


Table 1. Relative stabilities of different spin states of Fe-Zn doped on graphtriyne quantum dot (energies in eV).

System	Most Stable	2 nd Stable	3 rd Stable	4 th Stable
Fe@GTY	0.00 (<i>Quintet</i>)	1.94 (<i>Triplet</i>)	2.41 (<i>Septet</i>)	3.34 (<i>Singlet</i>)
Co@GTY	0.00 (<i>Doublet</i>)	1.37 (<i>Quartet</i>)	2.62 (<i>Sextet</i>)	5.52 (<i>Octet</i>)
Ni@GTY	0.00 (<i>Singlet</i>)	1.68 (<i>Triplet</i>)	3.95 (<i>Quintet</i>)	7.19 (<i>Septet</i>)
Cu@GTY	0.00 (<i>Doublet</i>)	0.98 (<i>Quartet</i>)	5.51 (<i>Sextet</i>)	7.97 (<i>Octet</i>)
Zn@GTY	0.00 (<i>Singlet</i>)	3.34 (<i>Triplet</i>)	6.89 (<i>Quintet</i>)	9.89 (<i>Septet</i>)

while Ni@GTY and Zn@GTY exhibits singlet as the most stable spin state. For Co@GTY and Cu@GTY complexes, doublet is the most stable spin multiplicity. Additionally, vibrational analysis was conducted to confirm that there are no imaginary frequencies in the optimized geometries of the designed SACs and all the reported structures represent true minima on the potential energy surface.

Table 2. Interaction energies (E_{int} in kcal mol⁻¹), HOMO energies (E_{HOMO} in eV), LUMO energies (E_{LUMO} in eV), and HOMO–LUMO gap (E_{gap} in eV).

System	E_{int}	E_{HOMO}	E_{LUMO}	E_{gap}
GTY	—	-6.68	-1.89	4.79
Fe@GTY	-76.35	-4.46	-1.93	2.53
Co@GTY	-5.97	-6.70	-1.91	4.78
Ni@GTY	-78.25	-6.23	-1.82	4.40
Cu@GTY	-4.78	-4.70	-1.91	2.79
Zn@GTY	-3.40	-6.09	-1.91	4.18

To evaluate the thermodynamic stability of the transition-metal@graphtriene single atom catalysts (TM@GTY SACs), we computed the interaction energies of Fe-Zn embedded graphtriene composites. The results from table 2 reveals negative interaction energies for all TM@GTY SACs. The negative interaction energies are evidence for the thermodynamic stability of our designed SACs. Ni anchored on graphtriene (Ni@GTY) has the highest interaction energy of -78.25 kcal mol⁻¹. This is followed by Fe doped graphtriene (Fe@GTY) interaction energy of -76.35 kcal mol⁻¹. The interaction energy for Co@GTY, Cu@GTY, and Zn@GTY are -5.97 , -4.78 , and -3.40 kcal mol⁻¹. Ni@GTY and Fe@GTY SACs exhibit the most negative interaction energies, indicating a strong chemical interaction or chemisorption between the metal atom and the graphtriene quantum dot. Chemisorption entails a strong chemical bond formation between the adsorbate (transition metal atoms (Ni and Fe) in this case) and the substrate (graphtriene quantum dot). This process is largely dictated by the electronic structure compatibility and the associated orbital interactions between the two entities. The interaction energies serve as a pivotal metric for assessing this and the markedly negative interaction energies of Ni@GTY and Fe@GTY elucidate chemisorption. Ni almost certainly has a $nd^{10}(n+1)s^0$ configuration, and the empty s orbital allows it to bind strongly to the graphtriene surface. While Fe has unpaired d-electrons that can form stronger covalent bonds with the carbon atoms of the graphtriene quantum dot. The higher negative interaction energies of Ni@GTY and Fe@GTY SACs also reveals that these complexes are the most stable. While others suffer from low interaction energies, making them less stable as a result. The geometry of graphtriene quantum dot remained unaffected from the doping of transition metals except for Ni@GTY in which the GTY structure is slightly distorted. The Ni atom has a small interaction distance with the graphtriene quantum dot and interacts strongly with neighboring carbon atoms causing distortion in the graphtriene geometry around the dopant.

To understand the influence of transition metal doping on the electronic properties of the graphtriene quantum dot, we performed a frontier molecular orbitals (FMO) analysis. This analysis allowed us to compute the energies of the highest occupied molecular orbital (HOMO) and the lowest unoccupied molecular orbital (LUMO) and to visualize their isodensities. The HOMO–LUMO energy gap, which is the energy difference between these two orbitals, is an important parameter in determining the electronic conductivity of a material. The FMO analysis provides a detailed understanding of the electronic structures of the transition metal doped graphtriene quantum dots and thus enables the evaluation of the influence of transition metal doping on the graphtriene. From figure 2, Pi orbitals are present in both the HOMO and LUMO levels of the pure graphtriene. The electronic density of the HOMO of the Ni@GTY reveals presence of the xy type of d orbital on the Ni atom. While Co@GTY does not have any HOMO density on the metal. Fe@GTY, Cu@GTY, and Zn@GTY contain s-orbital density in their HOMO on the metal atoms. The analysis of the lowest unoccupied molecular orbital (LUMO) revealed that, except for Ni, none of the other transition metals introduce any electronic density to the graphtriene quantum dot. The density of the GTY remains unchanged after the doping of a single metal atom. However, in the case of Ni@GTY, the density is concentrated on the side of the GTY that contains the Ni single metal atom. This suggests that the doping of Ni single metal atom perturbs the electronic density distribution in the LUMO of the graphtriene.

The analysis of the electronic properties of the pristine graphtriene quantum dot ($C_{54}H_{14}$) revealed that the energy gap between the highest occupied molecular orbital (HOMO) and the lowest unoccupied molecular orbital (LUMO) (E_{gap}) is 4.79 eV. The HOMO and LUMO energies are -6.68 eV and -1.89 eV, respectively. However, upon doping with Fe and Cu transition metal atoms, the E_{gap} is significantly reduced. The greatest reduction in the energy gap is observed after doping with Fe atom. This reduction in the energy gap suggests that the Fe and Cu metal atoms significantly influence the electronic structure of the graphtriene quantum dot and could increase its electronic conductivity. The E_{gap} in case of Fe@GTY is reduced to 2.53 eV and for Cu@GTY E_{gap} is reduced to 2.79 eV. The E_{gap} remains almost unchanged (4.78 eV) in case of doping of Co atom. Slight reduction in the E_{gap} is observed for Ni@GTY (4.40 eV) and Zn@GTY (4.18 eV). The anchoring of Fe and Cu

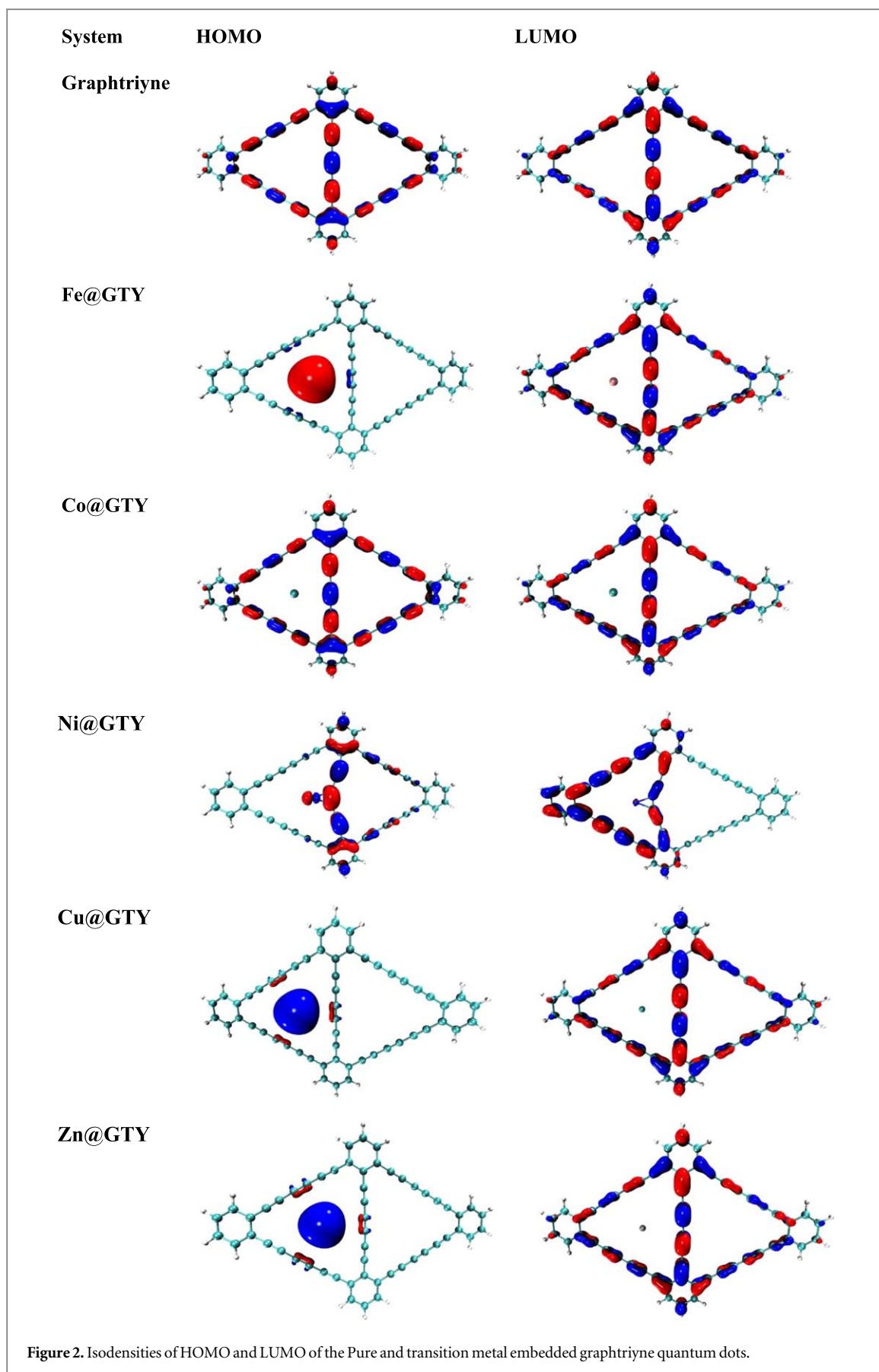
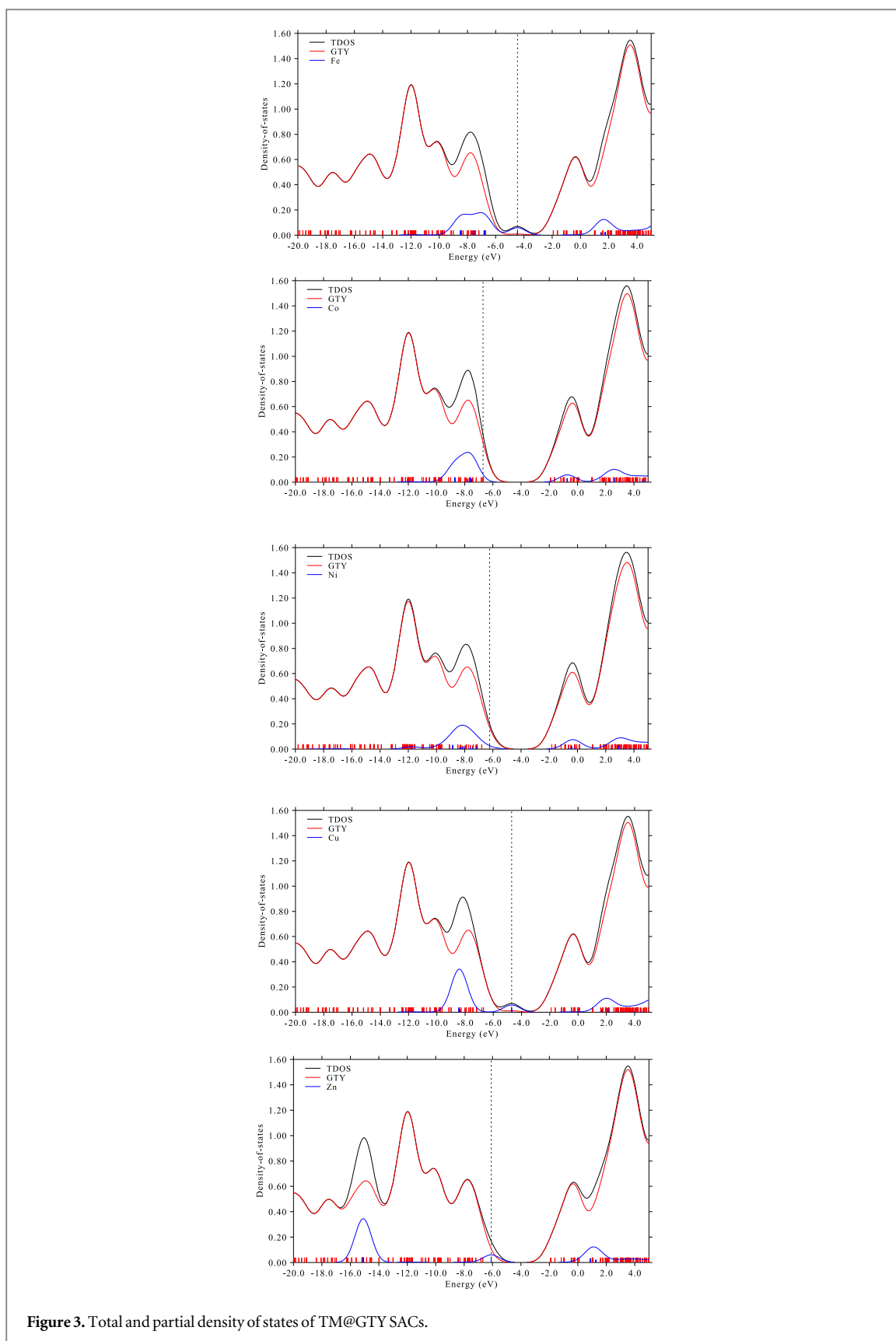


Figure 2. Isodensities of HOMO and LUMO of the Pure and transition metal embedded graphtriyne quantum dots.



single atoms results in an increase in the energy of the HOMO level, which is responsible for the significant narrowing of the E_{gap} of Fe@GTY and Cu@GTY SACs.

Figure 3 illustrates the TM@GTY complexes' total density of states (TDOS) as well as their partial density of states (PDOS). In the Fe@GTY, Cu@GTY, and Zn@GTY, the HOMO density is almost all concentrated on the single metal atom. The Ni atom in the Ni@GTY composite also has some contribution in the HOMO electronic

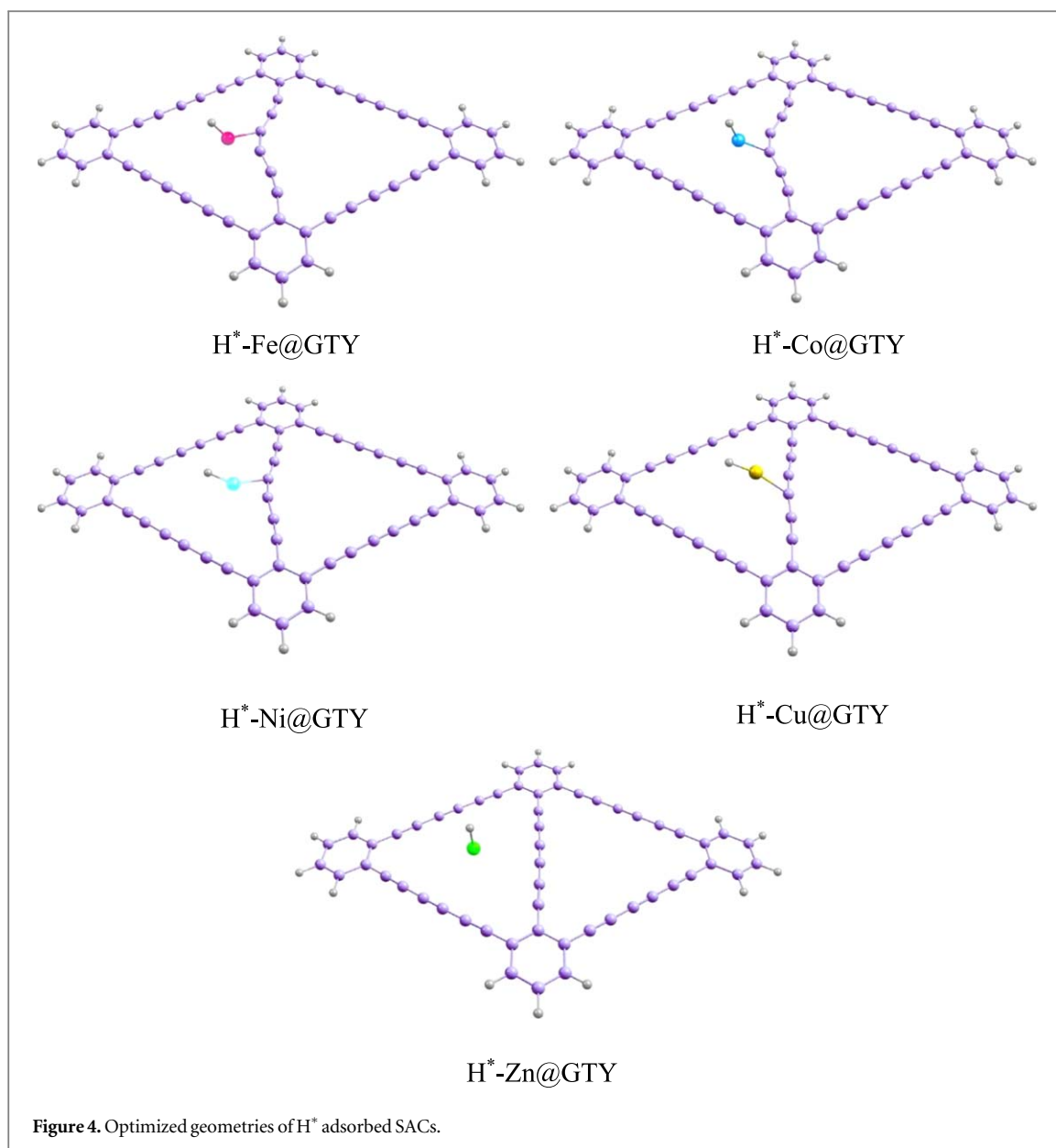


Table 3. Adsorption energies (E_{ad}), Free energy change of adsorbed H^* (ΔG_{H^*}), HOMO energies (E_{HOMO}), LUMO energies (E_{LUMO}), and HOMO–LUMO gap (E_{gap}). (All energies are in eV).

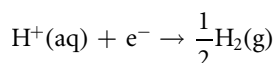
System	E_{ad}	ΔG_{H^*}	E_{HOMO}	E_{LUMO}	E_{gap}
$H^* - Fe@GTY$	−2.99	−2.39	−6.62	−1.86	4.76
$H^* - Co@GTY$	−3.26	−2.66	−6.54	−1.84	4.70
$H^* - Ni@GTY$	−1.90	−1.07	−6.72	−2.03	4.69
$H^* - Cu@GTY$	−3.53	−2.93	−6.70	−2.13	4.57
$H^* - Zn@GTY$	−0.81	−0.48	−5.15	−1.95	3.20

density. On the other hand, graphtriyne makes the most significant contribution to the occupied frontier molecular orbital in the Co@GTY, whereas transition metals' major contribution peaks appear at lower energy levels than HOMO.

Figure 4 illustrates the adsorption of atomic hydrogen on TM@GTY single atom catalysts, and table 3 provides a listing of the calculated adsorption energies for each of the catalysts. The computed adsorption energy for atomic hydrogen adsorption on Zn@GTY single atom catalyst is −0.81 eV, and as a result of its low hydrogen adsorption energy, it is anticipated that Zn@GTY will better catalyze the hydrogen evolution reaction. Ni@GTY

SAC has the second lowest adsorption energy for the adsorption of hydrogen (-1.90 eV). The computed atomic hydrogen adsorption energies on Fe@GTY, Co@GTY, and Cu@GTY are -2.99 eV, -3.26 eV, and -3.53 eV, respectively.

The hydrogen evolution reaction process is defined as follows under standard conditions:



The overall process of hydrogen evolution reaction (HER) is connected by the $\text{H}^+(\text{aq}) + \text{e}^-$, intermediate H^* and the product $\frac{1}{2}\text{H}_2(\text{g})$. Using the theoretical hydrogen electrode model, the chemical potential of the $\text{H}^+ + \text{e}^-$ pair can be determined by equating it to one half of the chemical potential of the hydrogen (H_2). Therefore, the free energy of atomic hydrogen adsorbed on the surface of the catalyst (ΔG_{H^*} of H^*) is considered as the key descriptor for assessing performance of the catalysts in hydrogen evolution reaction. This descriptor is essential for understanding the thermodynamic feasibility of the HER process and the ability of the electrocatalyst to facilitate the adsorption and desorption of hydrogen atoms. The following expression describes the change in hydrogen's free energy in its adsorbed state:

$$\Delta G_{\text{H}^*} = E_{\text{ad}} + \Delta E_{\text{ZPE}} - T\Delta S_{\text{H}}$$

Here H^* represents the adsorbed hydrogen, E_{ad} represents the adsorption energy of hydrogen, and ΔE_{ZPE} represents the change in zero-point energy between the adsorbed and gaseous forms of hydrogen. Additionally, the term ($T\Delta S_{\text{H}}$) accounts for the entropy contribution of adsorbed hydrogen at a temperature of 298 K. It is essential to understand the thermodynamic factors that influence the adsorption of atomic hydrogen on the catalyst surface to optimize the catalytic activity of materials for the hydrogen evolution reaction.

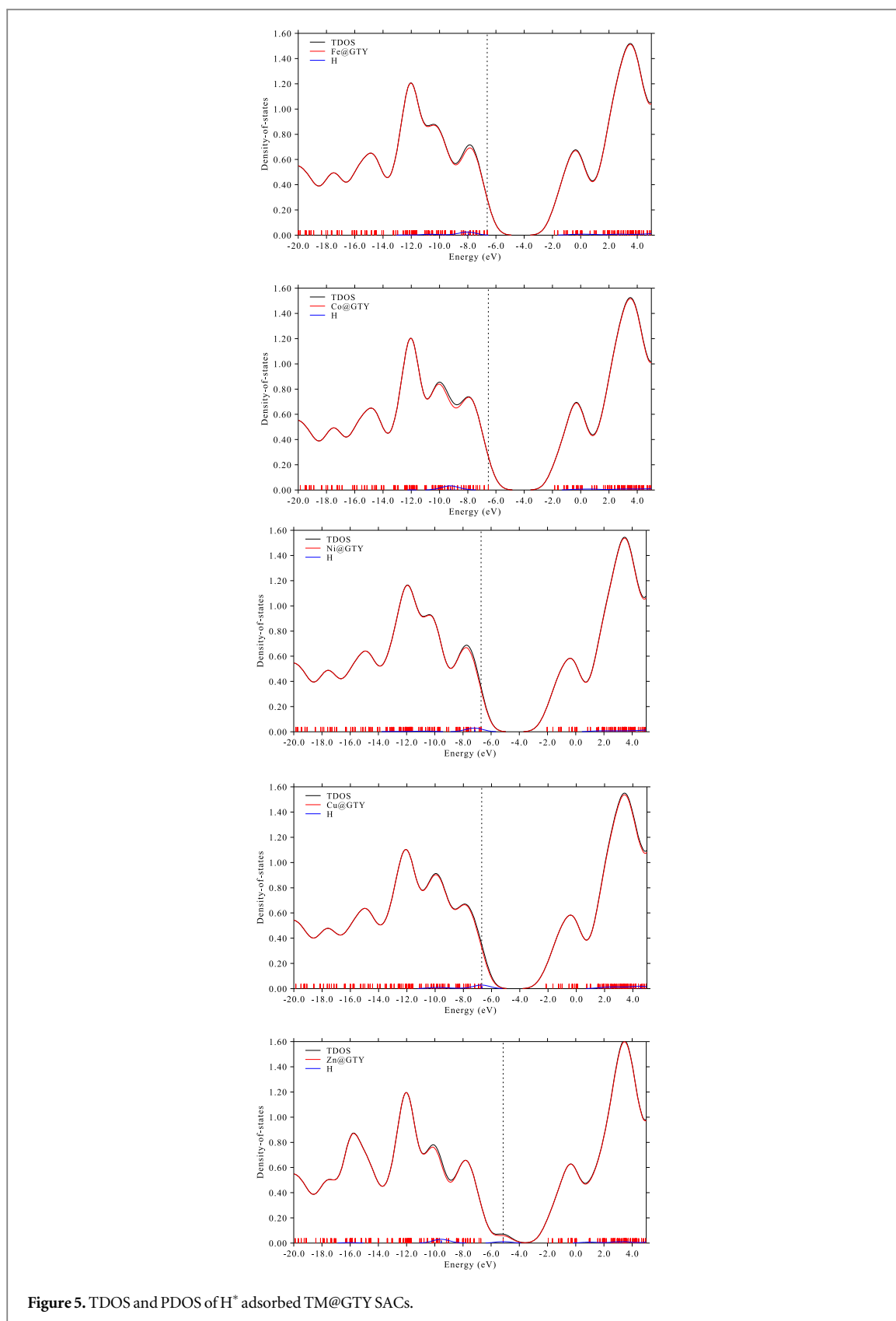
A high value for ΔG_{H^*} in the positive range implies that the process of adsorbing hydrogen onto the catalyst surface is energetically unfavorable. Conversely, a high value for ΔG_{H^*} in the negative range implies that the process of releasing adsorbed hydrogen from the catalyst is energetically challenging. High values of ΔG_{H^*} in both positive and negative range inhibit the activity of the HER catalyst. Therefore, for an efficient HER electrocatalyst, the value of ΔG_{H^*} should be as close to zero as possible. In this study, we estimated ΔG_{H^*} of hydrogen adsorption on TM@GTY single atom catalysts to determine the HER catalytic response of transition metal SACs anchored on graphtriyne. This allowed us to evaluate the HER catalytic performance of the proposed catalysts and identify the most promising candidates for efficiently catalyzing the HER process.

From table 3, since the ΔG_{H^*} value of Zn@GTY (-0.48 eV) is closer to the ideal value ($\Delta G_{\text{H}^*} = 0$ eV), the adsorption of hydrogen and the release of hydrogen from the catalyst surface will be an easy and efficient process. This is because the ΔG_{H^*} value of Zn@GTY is closer to the ideal value for HER process. As a result, the optimum catalytic performance for the HER process is provided by the Zn single atom anchored on graphtriyne quantum dot. Ni@GTY catalyst has also low ΔG_{H^*} value (-1.07 eV). Therefore, Ni@GTY can also show better catalytic activity for HER. Our findings indicate that Zn@GTY and Ni@GTY single atom catalysts exhibit superior HER catalytic performance when compared to other catalysts such as hydrogen on coronene and pyrene polycyclic aromatic hydrocarbons (PAHs), as their reported adsorption energies fall within the range of $0.6-1.4$ and $0.6-1.6$ eV, respectively [59]. These results suggest that Zn@GTY and Ni@GTY SACs may be considered as promising candidates for effectively catalyzing the hydrogen evolution reaction. The superior performance of these catalysts highlights the potential of graphtriyne quantum dot as a support material and transition metal atoms as single atom centers for the development of highly efficient and low-cost electrocatalysts for the hydrogen evolution reaction.

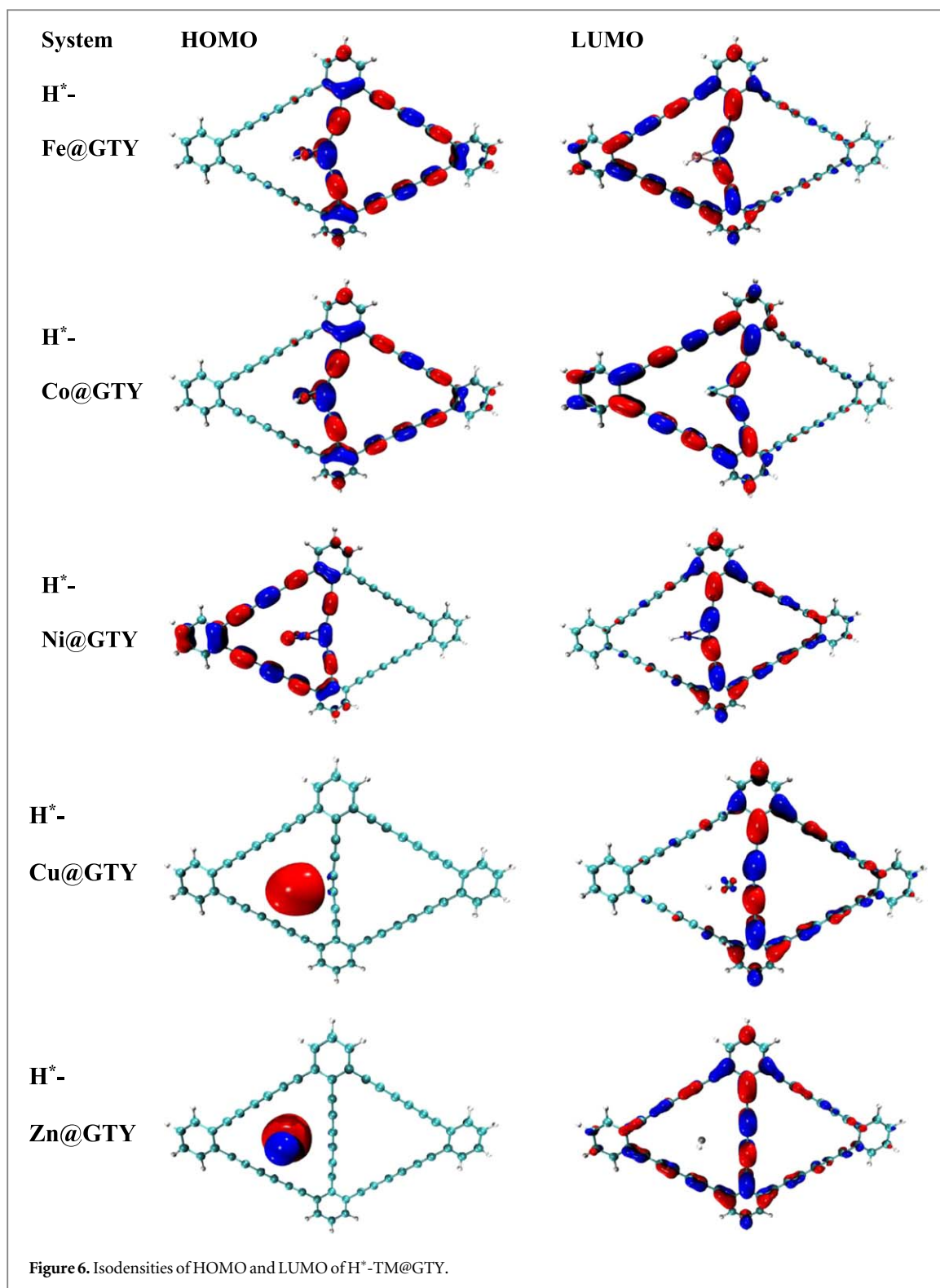
The estimated ΔG_{H^*} values for Fe@GTY, Co@GTY, and Cu@GTY are -2.39 eV, -2.66 eV, and -2.93 eV, respectively. These high negative values of ΔG_{H^*} suggests that hydrogen is chemisorbed and that the process of releasing it is difficult. As a result, the Fe@GTY, Co@GTY, and Cu@GTY have poor efficiency for HER catalysis.

In comparison with existing literature on metal-doped graphynes, our study on metal@GTY catalysts builds upon the foundational works reviewed by Li *et al*, [60] and Song *et al*, [61] who primarily focus on metal@GDY catalysts. Our findings align with previous investigations into the electrocatalytic benefits of metal-doping in graphyne and its analogues. Specifically, our work can be contextualized alongside the research conducted by Xue *et al* in 2018, where Ni^0/GDY and Fe^0/GDY electrocatalysts were synthesized and evaluated for their hydrogen evolution reaction (HER) performance [62]. Xue *et al* reported high catalytic activities for both Ni^0/GDY and Fe^0/GDY . In our study, Ni@GTY also demonstrated improved HER performance, corroborating the findings of Xue *et al*. However, it is noteworthy that Fe@GTY exhibited suboptimal activity for HER in our system, diverging from the high performance observed for Fe^0/GDY in their study. This discrepancy potentially highlights the sensitivity of HER performance to the specific structure and electronic configurations of the graphyne framework.

In order to investigate the interaction between the adsorbed H^* and the TM@GTY single atom catalysts, we conducted density of states (DOS) and frontier molecular orbitals (FMO) analyses. Figure 5 shows the DOS



spectra of the H* -TM@GTY complexes, and figure 6 provides a graphical representation of the frontier molecular orbitals (HOMO and LUMO). The interaction between the H* and TM@GTY SACs leads to variations in the HOMO–LUMO energy gap (E_{gap}) and in the DOS spectrum. The DOS spectra of the H* -TM@GTY complexes clearly show that, after hydrogen adsorption, additional peaks appear for hydrogen at the Fermi level or slightly below it, indicating the adsorption of H* on the TM@GTY.



As a result of the interaction between H* and the Zn@GTY catalyst, the HOMO–LUMO gap (E_{gap}) is significantly reduced from 4.18 eV to 3.20 eV. Conversely, the E_{gap} for Fe@GTY and Cu@GTY is significantly widened after the adsorption of hydrogen while slight variations in E_{gap} is observed for Co@GTY and Ni@GTY. As can be seen in the illustration of the HOMO orbital of H* -Ni@GTY, H* -Cu@GTY, and H* -Zn@GTY complexes, both the adsorbed H* atom and the metal atom have HOMO orbital's electronic density. However, in the case of H* -Cu@GTY and H* -Zn@GTY complexes, there is no HOMO orbital's electronic density on the graphtriyne. For H* -Fe@GTY and H* -Co@GTY complexes, the HOMO orbital's electronic density is completely from the TM@GTY and absent from the adsorbed hydrogen.

4. Conclusions

This study employed first principles density functional theory simulations to investigate the potential of single transition metal atoms anchored on graphtriyne quantum dots as catalysts for the hydrogen evolution reaction (HER). By utilizing five transition metals (Fe, Co, Ni, Cu, and Zn) as single atom centers and graphtriyne quantum dot as a support material, we designed a series of single atom catalysts (SACs) and examined their electronic structures and HER catalytic performance. Our results indicate that the TM@GTY SACs exhibit good stability, with the highest interaction energy observed for Ni@GTY SAC ($-78.25 \text{ kcal mol}^{-1}$) followed by Fe@GTY ($-76.35 \text{ kcal mol}^{-1}$). Furthermore, the Zn@GTY and Ni@GTY SACs displayed excellent HER performance, with small ΔGH^* values of -0.48 eV and -1.07 eV , respectively. These findings suggest that transition metal atoms supported on graphtriyne quantum dot may be a promising approach for the development of low-cost HER catalysts. The results of this study may pave the way for further exploration of this class of catalysts for hydrogen production.

Acknowledgments


M Imran expresses his appreciation to the Deanship of Scientific Research at King Khalid University, Saudi Arabia, for funding this work through research group program under grant number R.G.P. 2/522/44. The authors also acknowledge the Higher Education Commission of Pakistan, COMSATS University, Abbottabad Campus and University of Bahrain for financial support.

Data availability statement

The data cannot be made publicly available upon publication because they are owned by a third party and the terms of use prevent public distribution. The data that support the findings of this study are available upon reasonable request from the authors.

ORCID iDs

Faizan Ullah  <https://orcid.org/0000-0002-3398-9412>

Mazhar Amjad Gilani  <https://orcid.org/0000-0003-0366-4374>

Tariq Mahmood  <https://orcid.org/0000-0001-8850-9992>

References

- [1] Lin H, Liu N, Shi Z, Guo Y, Tang Y and Gao Q 2016 Cobalt-doping in molybdenum-carbide nanowires toward efficient electrocatalytic hydrogen evolution *Adv. Funct. Mater.* **26** 5590–8
- [2] Wen C, Chen L, Xie Y, Bai J and Liang X 2021 MOF-derived carbon-containing Fe doped porous CoP nanosheets towards hydrogen evolution reaction and hydrodesulfurization *Int. J. Hydrogen Energy* **46** 33420–8
- [3] Nithya V D 2021 Recent advances in CoSe₂ electrocatalysts for hydrogen evolution reaction *Int. J. Hydrogen Energy* **46** 36080–102
- [4] Huang X, Xu X, Luan X and Cheng D 2020 CoP nanowires coupled with CoMoP nanosheets as a highly efficient cooperative catalyst for hydrogen evolution reaction *Nano Energy* **68** 104332
- [5] Zou X and Zhang Y 2015 Noble metal-free hydrogen evolution catalysts for water splitting *Chem. Soc. Rev.* **44** 5148–80
- [6] Dresselhaus M S and Thomas I L 2001 Alternative energy technologies *Nature* **414** 332–7
- [7] Safizadeh F, Ghali E and Houlachi G 2015 Electrocatalysis developments for hydrogen evolution reaction in alkaline solutions—A Review *Int. J. Hydrogen Energy* **40** 256–74
- [8] Zhao G, Rui K, Dou S X and Sun W 2018 Heterostructures for Electrochemical Hydrogen Evolution Reaction: A Review *Adv. Funct. Mater.* **28** 1803291
- [9] Eftekhari A 2017 Electrocatalysts for hydrogen evolution reaction *Int. J. Hydrogen Energy* **42** 11053–77
- [10] Shen Y, Zhou Y, Wang D, Wu X, Li J and Xi J 2018 Nickel–Copper Alloy Encapsulated in Graphitic Carbon Shells as Electrocatalysts for Hydrogen Evolution Reaction. *Advanced Energy Materials*. **8** 1701759
- [11] Zhao J, Tran P D, Chen Y, Loo J S C, Barber J and Xu Z J 2015 Achieving high electrocatalytic efficiency on copper: a low-cost alternative to platinum for hydrogen generation in water *ACS Catal.* **5** 4115–20
- [12] Zeng Z, Chang K-C, Kubal J, Markovic N M and Greeley J 2017 Stabilization of ultrathin (hydroxy)oxide films on transition metal substrates for electrochemical energy conversion *Nat. Energy* **2** 17070
- [13] Jiao Y, Zheng Y, Jaroniec M and Qiao S Z 2015 Design of electrocatalysts for oxygen- and hydrogen-involving energy conversion reactions *Chem. Soc. Rev.* **44** 2060–86
- [14] Badrnezhad R, Nasri F, Pourfarzad H and Jafari S K 2021 Effect of iron on Ni–Mo–Fe composite as a low-cost bifunctional electrocatalyst for overall water splitting *Int. J. Hydrogen Energy* **46** 3821–32
- [15] Greeley J, Jaramillo T F, Bonde J, Chorkendorff I and Nørskov J K 2006 Computational high-throughput screening of electrocatalytic materials for hydrogen evolution *Nat. Mater.* **5** 909–13
- [16] Ledendecker M, Krick Calderón S, Papp C, Steinrück H-P, Antonietti M and Shalom M 2015 The Synthesis of Nanostructured Ni₅P₄ Films and their Use as a Non-Noble Bifunctional Electrocatalyst for Full Water Splitting *Angew. Chem. Int. Ed.* **54** 12361–5

- [17] Du H, Kong R-M, Guo X, Qu F and Li J 2018 Recent progress in transition metal phosphides with enhanced electrocatalysis for hydrogen evolution *Nanoscale*. **10** 21617–24
- [18] Chia X and Pumera M 2018 Layered transition metal dichalcogenide electrochemistry: journey across the periodic table *Chem. Soc. Rev.* **47** 5602–13
- [19] Majhi K C and Yadav M 2020 Transition metal chalcogenides based nanocomposites as efficient electrocatalyst for hydrogen evolution reaction over the entire pH range *Int. J. Hydrogen Energy* **45** 24219–31
- [20] Song R, Li D, Xu Y, Gao J, Wang L and Li Y 2022 Interface engineering of heterogeneous transition metal chalcogenides for electrocatalytic hydrogen evolution *Nanoscale Adv.* **4** 865–70
- [21] Tiwari A P, Novak T G, Bu X, Ho J C and Jeon S 2018 Layered Ternary and Quaternary Transition Metal Chalcogenide Based Catalysts for Water Splitting *Catalysts*. **8** 551
- [22] Askari M B, Salarizadeh P, Rozati S M and Seifi M 2019 Two-dimensional transition metal chalcogenide composite/reduced graphene oxide hybrid materials for hydrogen evolution application *Polyhedron* **162** 201–6
- [23] Peng X, Pi C, Zhang X, Li S, Huo K and Chu P K 2019 Recent progress of transition metal nitrides for efficient electrocatalytic water splitting *Sustainable Energy & Fuels*. **3** 366–81
- [24] Abghoui Y and Skúlason E 2017 Hydrogen evolution reaction catalyzed by transition-metal nitrides *The J. Phys. Chem. C* **121** 24036–45
- [25] Wang H et al 2021 Transition metal nitrides for electrochemical energy applications *Chem. Soc. Rev.* **50** 1354–90
- [26] Cheng N, Zhang L, Doyle-Davis K and Sun X 2019 *Single-Atom Catalysts: From Design to Application. Electrochemical Energy Reviews*. **2** 539–73
- [27] Shen Z et al 2020 3d transitional-metal single atom catalysis toward hydrogen evolution reaction on MXenes supports *Int. J. Hydrogen Energy* **45** 14396–406
- [28] Wang A, Li J and Zhang T 2018 Heterogeneous single-atom catalysis *Nature Reviews Chemistry*. **2** 65–81
- [29] Xiao C et al 2021 High-throughput screening of transition metal single-atom catalyst anchored on Janus MoSSe basal plane for hydrogen evolution reaction *Int. J. Hydrogen Energy* **46** 10337–45
- [30] Sun Z, Gao Z, Zhang C, Guan L and Tao J 2021 Atomically dispersed low-cost transition metals catalyze efficient hydrogen evolution on two-dimensional SnO nanosheets *Int. J. Hydrogen Energy* **46** 28602–12
- [31] Alarawi A, Ramalingam V and He J-H 2019 Recent advances in emerging single atom confined two-dimensional materials for water splitting applications *Materials Today Energy* **11** 1–23
- [32] Lin X, Ng S-F and Ong W-J 2022 Coordinating single-atom catalysts on two-dimensional nanomaterials: A paradigm towards bolstered photocatalytic energy conversion *Coord. Chem. Rev.* **471** 214743
- [33] Xu Q, Zhang J, Wang D and Li Y 2021 Single-atom site catalysts supported on two-dimensional materials for energy applications *Chin. Chem. Lett.* **32** 3771–81
- [34] Back S and Jung Y 2017 TiC- and TiN-Supported single-atom catalysts for dramatic improvements in CO₂ electrochemical reduction to CH₄ *ACS Energy Lett.* **2** 969–75
- [35] Wang J et al 2019 Enhancing activity and reducing cost for electrochemical reduction of CO₂ by supporting palladium on metal carbides *Angew. Chem. Int. Ed.* **58** 6271–5
- [36] Zhao C-X, Zhang G-X, Gao W and Jiang Q 2019 Single metal atoms regulated flexibly by a 2D InSe substrate for CO₂ reduction electrocatalysts *J. Mater. Chem. A* **7** 8210–7
- [37] Xu G, Wang R, Ding Y, Lu Z, Ma D and Yang Z 2018 First-principles study on the single Ir atom embedded graphdiyne: An efficient catalyst for CO oxidation *The J. Phys. Chem. C* **122** 23481–92
- [38] Wang Z, Zhao J and Cai Q 2017 CO₂ electroreduction performance of a single transition metal atom supported on porphyrin-like graphene: a computational study *Phys. Chem. Chem. Phys.* **19** 23113–21
- [39] Lim D-H, Jo J H, Shin D Y, Wilcox J, Ham H C and Nam S W 2014 Carbon dioxide conversion into hydrocarbon fuels on defective graphene-supported Cu nanoparticles from first principles *Nanoscale*. **6** 5087–92
- [40] Zhang X, Sun S and Wang S 2020 First-principles investigation on the bonding mechanisms of two-dimensional carbon materials on the transition metals surfaces *RSC Adv.* **10** 43412–9
- [41] Neese F, Wennmohs F, Becker U and Riplinger C 2020 The ORCA quantum chemistry program package *The J. Chem. Phys.* **152** 224108
- [42] Neese F 2012 The ORCA program system *WIREs Computational Molecular Science*. **2** 73–8
- [43] Lin Y-S, Li G-D, Mao S-P and Chai J-D 2013 Long-range corrected hybrid density functionals with improved dispersion corrections *J. Chem. Theory Comput.* **9** 263–72
- [44] Weigend F and Ahlrichs R 2005 Balanced basis sets of split valence, triple zeta valence and quadruple zeta valence quality for H to Rn: Design and assessment of accuracy *Phys. Chem. Chem. Phys.* **7** 3297–305
- [45] Neese F, Wennmohs F, Hansen A and Becker U 2009 Efficient, approximate and parallel Hartree–Fock and hybrid DFT calculations. A ‘chain-of-spheres’ algorithm for the Hartree–Fock exchange *Chem. Phys.* **356** 98–109
- [46] Weigend F 2006 Accurate Coulomb-fitting basis sets for H to Rn *Phys. Chem. Chem. Phys.* **8** 1057–65
- [47] Goerigk L and Grimme S 2011 Efficient and accurate Double-Hybrid-Meta-GGA density Functionals—Evaluation with the extended GMTKN30 database for general main group thermochemistry, kinetics, and noncovalent interactions *J. Chem. Theory Comput.* **7** 291–309
- [48] Hellweg A, Hättig C, Höfener S and Klopper W 2007 Optimized accurate auxiliary basis sets for RI-MP2 and RI-CC2 calculations for the atoms Rb to Rn *Theor. Chem. Acc.* **117** 587–97
- [49] Steinmetz M and Grimme S 2013 Benchmark study of the performance of density functional theory for bond activations with (Ni,Pd)-Based transition-metal catalysts *ChemistryOpen*. **2** 115–24
- [50] Grimme S, Antony J, Ehrlich S and Krieg H 2010 A consistent and accurate *ab initio* parametrization of density functional dispersion correction (DFT-D) for the 94 elements H–Pu *J. Chem. Phys.* **132** 154104
- [51] Grimme S, Ehrlich S and Goerigk L 2011 Effect of the damping function in dispersion corrected density functional theory *J. Comput. Chem.* **32** 1456–65
- [52] Lu T and Chen F 2012 Multiwfn: A multifunctional wavefunction analyzer *J. Comput. Chem.* **33** 580–92
- [53] Humphrey W, Dalke A and Schulten K 1996 VMD: Visual molecular dynamics *J. Mol. Graphics* **14** 33–8
- [54] Yusran L O, Asih R and Arifin R 2021 Darminto. Effect of vacancy defects on electronic band structure and magnetic moment of single-layered graphene: a density functional theory study *Journal of Physics: Conference Series* 1951, 012013
- [55] Gao Y, Xu D, Cui T and Li D 2021 Stability of hydrogen-terminated graphene edges *Phys. Chem. Chem. Phys.* **23** 13261–6
- [56] Hanwell M D, Curtis D E, Lonie D C, Vandermeersch T, Zurek E and Hutchison G R 2012 Avogadro: an advanced semantic chemical editor, visualization, and analysis platform *Journal of Cheminformatics*. **4** 1–17

- [57] Jana S, Bandyopadhyay A and Jana D 2019 Acetylenic linkage dependent electronic and optical behaviour of morphologically distinct '-ynes' *Phys. Chem. Chem. Phys.* **21** 13795–808
- [58] Bartolomei M, Carmona-Novillo E and Giorgi G 2015 First principles investigation of hydrogen physical adsorption on graphynes' layers *Carbon* **95** 1076–81
- [59] Rasmussen J A, Henkelman G and Hammer B 2011 Pyrene: Hydrogenation, hydrogen evolution, and π -band model *The J. Chem. Phys.* **134** 164703
- [60] Li J, Gao X, Zhu L, Ghazzal M N, Zhang J, Tung C-H and Wu L-Z 2020 Graphdiyne for crucial gas involved catalytic reactions in energy conversion applications *Energy Environ. Sci.* **13** 1326–46
- [61] Song B *et al* 2020 Using graphdiyne (GDY) as a catalyst support for enhanced performance in organic pollutant degradation and hydrogen production: A review *J. Hazard. Mater.* **398** 122957
- [62] Xue Y *et al* 2018 Anchoring zero valence single atoms of nickel and iron on graphdiyne for hydrogen evolution *Nat. Commun.* **9** 1460